Pergamon

Int. J. Heat Mass Transfer. Vol. 38, No. 8, pp. 1517–1525, 1995

0017-9310/95 $9.50+0.00

0017-9310(94)00340-8

Conjugate mixed convection on a vertical surface in a porous medium

I. POP
Faculty of Mathematics, University of Cluj, R-3400 Cluj, CP 253, Romania

and

D. LESNIC and D. B. INGHAM
Department of Applied Mathematical Studies, University of Leeds, Leeds LS2 9JT, U.K.

(*Received* 19 *January* 1994)

Abstract—The aim of this paper is to present a detailed analysis of the problem of steady conjugate mixed-convection flow along a vertical finite flat plate which is embedded in a porous medium under the boundary-layer approximation. The problem then reduces to a parabolic partial differential equation which involves only the buoyancy parameter, λ. The cases of both aiding ($\lambda > 0$) and opposing ($\lambda < 0$) flows are considered. Full numerical and asymptotic solutions are obtained over a wide range of values of λ and the results for the temperature profiles on the plate and in the convective fluid are presented. It is found that, unlike *all* other problems previously investigated, in both a porous and a non-porous medium and for all inclinations of the plate, unseparated flows can be obtained in this *conjugate* situation even when there is an opposing flow when $\lambda \geqslant -1$. Further, when λ is very large and negative, predictions of the separation point of the boundary layer from the plate are also reported.

1. INTRODUCTION

The problems which occur in conjugate free and forced convection from vertical and horizontal surfaces in a viscous fluid have been the concern of researchers for more than 30 years (see, for example, the recent review article by Martynenko and Sokovishin [1]). However, very little research work has been performed on the corresponding porous medium configuration [2, 3]. In the mixed-convection region it is important to study such problems because frequently the boundary layer separates, which has a considerable effect on the heat transfer characteristics.

In this paper we present an analysis of the problem of conjugate mixed convection from a vertical finite flat plate which is embedded in a porous medium. We propose new non-dimensional co-ordinates which are such that the conjugation parameter is scaled from the governing equations. Thereby, the problem depends only on one parameter, namely the buoyancy parameter, λ, which is the ratio of the Rayleigh to the Peclet number, Ra/Pe. Both the situation when the flow and buoyancy force are in the same direction, which is referred to as assisting flow, and that when they are in opposite directions, which is referred to as opposing flow, are discussed. It is worth mentioning that, in all cases previously investigated, in both a porous medium and a non-porous medium, it has always been found that, when there is an opposing flow, no matter what the inclination of the plate, the boundary layer separates at some distance along the plate. However, in the present *conjugate* problem the flow does not separate for $\lambda \geqslant -1$, i.e. there is a regime in which the flow does not separate even though the flow is opposing in nature. When $\lambda < -1$ the flow does separate and the separation point has been determined from the full numerical solution. It is found that, as one would have physically predicted, the smaller the value of λ the sooner flow separates. When λ is very large and negative an estimate of the distance along the plate where the flow separates is presented. Further, in this paper we predict the temperature fields both in the boundary layer adjacent to the plate and at the solid–fluid interface, which are determined by the common solution of the energy equations for the fluid and the solid, respectively.

2. GOVERNING EQUATIONS

The co-ordinate system and flow variables are shown in a schematic diagram (Fig. 1). The model is based on a vertical rectangular plate, of length l and thickness b, which is embedded in a porous medium and over which the fluid flows with an undistorted uniform speed U_∞. The outside surface of the plate is maintained at a constant temperature T_0, while the ambient fluid is at a uniform temperature T_∞, where $T_0 > T_\infty$ (aiding flow) or $T_0 < T_\infty$ (opposing flow). We assume that the boundary-layer approximation holds in the convective fluid and that the plate is thin relative to its length, i.e. $b/l \ll 1$, so that the axial

NOMENCLATURE

b	thickness of the plate
g	acceleration due to gravity
k_f	effective thermal conductivity of the convective fluid
k_s	thermal conductivity of the plate
K	permeability of the porous medium
l	length of the plate
L	characteristic length scale, $[g\beta K\lvert T_0-T_\infty\rvert/(\nu\alpha)](bk_s/k_f)^2$
Pe	Peclet number, $U_\infty L/\alpha$
Ra	Rayleigh number, $g\beta K(T_0-T_\infty)L/(\nu\alpha)$
T	temperature in the convective fluid
T_0	temperature (constant) at the outer edge of the plate
T_∞	ambient temperature (constant)
T_w	temperature at the interface of the plate and convective fluid
$\bar{u}, \bar{v}$	velocity components along $\bar{x}$-, $\bar{y}$-axes
u_w	velocity on the plate
U_∞	free stream velocity (constant)
$\bar{x}, \bar{y}$	Cartesian co-ordinates along and normal to the plate.

Greek symbols

α	effective thermal diffusivity of saturated porous medium
β	coefficient of thermal expansion
η	pseudo-similarity variable
θ	non-dimensional temperature, $(T-T_\infty)/\lvert T_0-T_\infty\rvert$
θ_w	non-dimensional plate temperature
λ	buoyancy parameter, Ra/Pe
ν	kinematic viscosity of fluid
ξ	variable, $x^{1/2}$
ψ	non-dimensional stream function.

heat conduction in the solid plate can be neglected. Consequently the temperature profile in the plate can be assumed to be linear and thus we have (see, for example refs. [3, 4])

$$-k_f\left(\frac{\partial T}{\partial y}\right)_{y=0} = k_s(T_0-T_w)/b \tag{1}$$

where $T_w(x)$ is the temperature at the plate, which is

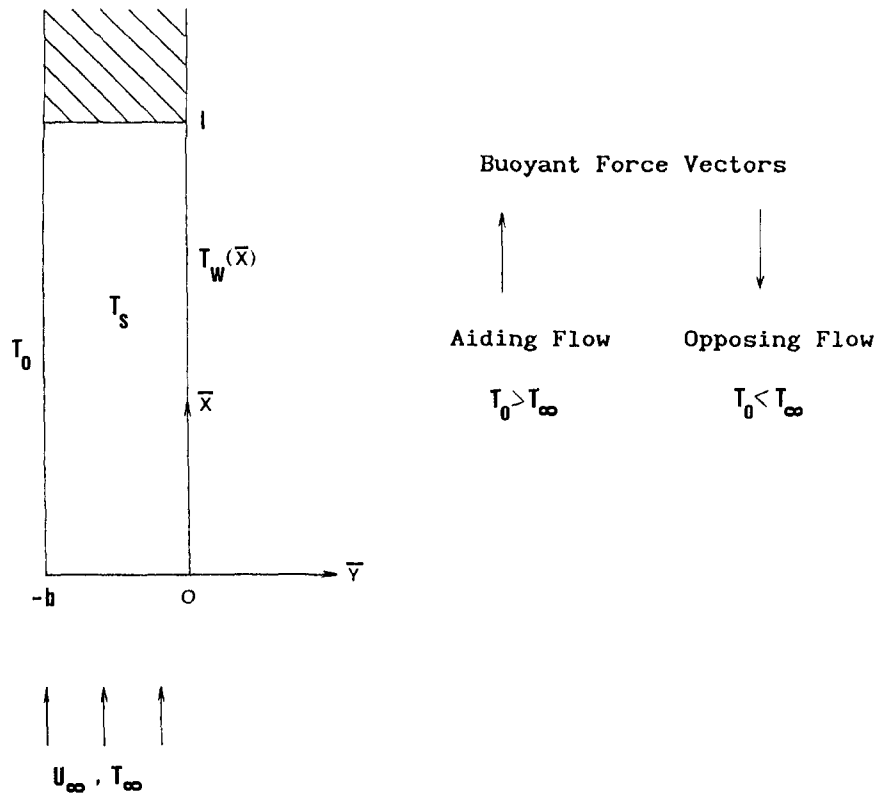

Fig. 1. Physical model and coordinate system.

not known *a priori* and is determined as part of the solution.

Using the Darcy and Boussinesq approximations the boundary-layer equations for the physical problem under consideration can be written in non-dimensional form as

$$\frac{\partial u}{\partial x}+\frac{\partial v}{\partial y}=0 \tag{2}$$

$$u=1+\lambda\theta \tag{3}$$

$$u\frac{\partial\theta}{\partial x}+v\frac{\partial\theta}{\partial y}=\frac{\partial^2\theta}{\partial y^2} \tag{4}$$

where the non-dimensional variables are defined as

$$x=\bar{x}/L \quad y=Pe^{1/2}\bar{y}/L \quad u=\bar{u}/U_\infty \tag{5a}$$

$$v=Pe^{1/2}\bar{v}/U_\infty \quad \theta=(T-T_\infty)/|T_0-T_\infty|. \tag{5b}$$

Here the parameter $\lambda=Ra/Pe$ represents the relative importance of the free to the forced convection, with $\lambda>0$ for the aiding case and $\lambda<0$ for the opposing case, $L=[g\beta K|T_0-T_\infty|/(\nu\alpha)](bk_s/k_f)^2$ is the characteristic length of the plate, $Ra=g\beta K(T_0-T_\infty)L/(\nu\alpha)$ is the Rayleigh number, and $Pe=U_\infty L/\alpha$ is the Peclet number.

The boundary conditions appropriate to this problem are

$$v=0 \quad \frac{\partial\theta}{\partial y}=\theta-1 \quad \text{on} \quad y=0 \tag{6a}$$

$$\theta=0 \quad \text{as} \quad y\to\infty. \tag{6b}$$

The system of equations (2)–(4) and the boundary conditions (6) only involve the single parameter λ. Further, the length of the plate l does not appear in the non-dimensional variables (5) and only enters the solution through the range of the validity of the solution, i.e.

$$0\leqslant x\leqslant\frac{\nu l}{U_\infty}\left(\frac{k_s}{bk_f}\right)^2. \tag{7}$$

3. SOLUTION

We first obtain a series solution which is valid near the leading edge of the surface of the plate in powers of $x^{1/2}$. We then obtain an asymptotic expansion which is valid for large x and $\lambda>0$. These two solutions are then joined by a numerical solution of the full boundary-layer equations.

3.1. *Solution for small* x

The transformed variables appropriate to this situation are

$$\psi=x^{1/2}f(x,\eta) \quad \theta=x^{1/2}h(x,\eta) \tag{8a}$$

where

$$\eta=y/x^{1/2}. \tag{8b}$$

Equations (3) and (4) then become

$$f'=1+\lambda x^{1/2}h \tag{9}$$

$$2h''+fh'-f'h=2x\left(f'\frac{\partial h}{\partial x}-h'\frac{\partial f}{\partial x}\right) \tag{10}$$

and boundary conditions (6) reduce to

$$f=0 \quad h'=x^{1/2}h-1 \quad \text{on} \quad \eta=0 \tag{11a}$$

$$h=0 \quad \text{as} \quad \eta\to\infty \tag{11b}$$

where primes denote partial differentiation with respect to η.

We look for the solution of equations (9) and (10), subject to the boundary conditions (11), in the form

$$f=f_0(\eta)+x^{1/2}f_1(\eta)+xf_2(\eta)+\ldots \tag{12a}$$

$$h=h_0(\eta)+x^{1/2}h_1(\eta)+xh_2(\eta)+\ldots \tag{12b}$$

where the coefficient functions are given by

$$f_0'=1$$

$$2h_0''+f_0h_0'-f_0'h_0=0$$

$$f_0(0)=0 \quad h_0'(0)=-1 \quad h_0(\infty)=0;$$

$$f_j'=\lambda h_{j-1} \tag{13}$$

$$2h_j''+f_0h_j'-(j+1)f_0'h_j=\sum_{i=0}^{j-1}[(i+1)h_if_{j-i}'-(i+2)f_{i+1}h_{j-i-1}']$$

$$f_j(0)=0 \quad h_j'(0)=h_{j-1}(0) \quad h_j(\infty)=0 \tag{14}$$

with $j\geqslant 1$. It should be noted that equations (13) describe the ordinary forced convection flow along a flat plate in a porous medium subject to a constant heat flux.

The exact solutions for f_0, h_0, f_1 and h_1 may be obtained in terms of the complementary error function, namely

$$f_0=\eta \tag{15a}$$

$$h_0=-\eta\,\mathrm{erfc}\,(\eta/2)+\frac{2}{\sqrt{\pi}}e^{-\eta^2/4}$$

$$f_1=\lambda\left[1+\frac{1}{\sqrt{\pi}}\eta e^{-\eta^2/4}-(1+\tfrac{1}{2}\eta^2)\,\mathrm{erfc}\,(\eta/2)\right]$$

$$h_1=(-1+\tfrac{3}{4}\lambda)\left[(1+\tfrac{1}{2}\eta^2)\,\mathrm{erfc}\,(\eta/2)-\frac{1}{\sqrt{\pi}}\eta e^{-\eta^2/4}\right]$$

$$+\lambda\left[\tfrac{1}{2}(1-\tfrac{1}{2}\eta^2)\,\mathrm{erfc}^2\,(\eta/2)\right.$$

$$\left.-\left(1-\frac{3}{2\sqrt{\pi}}\eta e^{-\eta^2/4}\right)\mathrm{erfc}\,(\eta/2)-\frac{2}{\pi}e^{-\eta^2/2}\right]. \tag{15b}$$

The non-dimensional temperature at the plate is then given, for small values of x, by

$$\theta_w^{(1)}(x) = \sum_{j=0}^{\infty} h_j(0) x^{(1+j)/2}. \quad (16)$$

3.2. *Solution for large* x

For this case one introduces the following variables:

$$\psi = x^{1/2}\tilde{f}(x,\tilde{\eta}) \quad \theta = \tilde{h}(x,\tilde{\eta}) \quad (17a)$$

where

$$\tilde{\eta} = y/x^{1/2}. \quad (17b)$$

Thus, equations (2) and (3) yield

$$\tilde{f}' = 1 + \lambda\tilde{h} \quad (18)$$

$$2\tilde{h}'' + \tilde{f}\tilde{h}' = 2x\left(\tilde{f}'\frac{\partial\tilde{h}}{\partial x} - \tilde{h}'\frac{\partial\tilde{f}}{\partial x}\right) \quad (19)$$

which has to be solved subject to boundary conditions (6), which become

$$\tilde{f} = 0 \quad x^{-1/2}\tilde{h}' = \tilde{h} - 1 \quad \text{on} \quad \tilde{\eta} = 0 \quad (20a)$$

$$\tilde{h} = 0 \quad \text{as} \quad \tilde{\eta} \to \infty \quad (20b)$$

where primes now denote partial differentiation with respect to $\tilde{\eta}$. The solution of equations (18)–(20) for large values of x is of the form

$$\tilde{f} = \tilde{f}_0(\tilde{\eta}) + x^{-1/2}\tilde{f}_1(\tilde{\eta}) + \ldots \quad (21a)$$

$$\tilde{h} = \tilde{h}_0(\tilde{\eta}) + x^{-1/2}\tilde{h}_1(\tilde{\eta}) + \ldots \quad (21b)$$

where the coefficient functions are determined from the following two sets of equations:

$$\begin{aligned} \tilde{f}_0' &= 1 + \lambda\tilde{h}_0 \\ 2\tilde{h}_0'' + \tilde{f}_0\tilde{h}_0' &= 0 \\ \tilde{f}_0(0) = 0 \quad \tilde{h}_0(0) &= 1 \quad \tilde{h}_0(\infty) = 0; \end{aligned} \quad (22)$$

$$\begin{aligned} \tilde{f}_1' &= \lambda\tilde{h}_1 \\ 2\tilde{h}_1' + \tilde{f}_0\tilde{h}_1 &= 0 \\ \tilde{h}_1(0) &= \tilde{h}_0'(0). \end{aligned} \quad (23)$$

Again, it is worth mentioning that equations (22) are equivalent to the equations of the non-conjugate mixed convection on an isothermal vertical flat plate which is embedded in a porous medium (see ref. [5]). The solution for the higher-order terms in the expansions (21) may similarly be obtained. However, we found (see ref. [6]) that at $0(x^{-1})$ the first eigensolution

$$\tilde{f}_e = \tilde{f}_0 - \tilde{\eta}\tilde{f}_0' \quad \tilde{h}_e = -\tilde{\eta}\tilde{h}_0 \quad (24)$$

arises due to the leading edge shift effect. Hence the usefulness of asymptotic expansion (21) is confined to terms up to $0(x^{-1})$.

The non-dimensional temperature at the plate for large values of x is then given by

$$\theta_w^{(2)}(x) = 1 - h_1(0)x^{-1/2} + \ldots. \quad (25)$$

3.3. *Numerical solution*

To obtain a solution which is valid for all values of x, equations (2)–(4) have been solved numerically using a finite-difference scheme [7] in combination with the method of continuous transformation [8]. Thus, we take

$$\psi = \xi F(\xi,\zeta) \quad \theta = \xi(1+\xi^2)^{-1/2}H(\xi,\zeta) \quad (26a)$$

where

$$\zeta = y/\xi \quad \xi = x^{1/2} \quad (26b)$$

and then equations (2)–(4) transform to

$$F' = 1 + \lambda\xi(1+\xi^2)^{-1/2}H \quad (27)$$

$$2H'' + FH' - \frac{1}{1+\xi^2}F'H = \xi\left(F'\frac{\partial H}{\partial\xi} - H'\frac{\partial F}{\partial\xi}\right) \quad (28)$$

and the boundary conditions (6) to

$$F = 0 \quad H' = \xi H - (1+\xi^2)^{1/2} \quad \text{on} \quad \zeta = 0 \quad (29a)$$

$$H = 0 \quad \text{as} \quad \zeta \to \infty. \quad (29b)$$

Primes now denote partial differential with respect to ζ. It should be noted that equations (27)–(29) reduce to equations (9)–(11) for small values of x and to equations (18)–(20) when x is large.

The non-dimensional temperature at the plate is now given by

$$\theta_w(\xi) = \xi(1+\xi^2)^{-1/2}H(\xi,0). \quad (30)$$

4. RESULTS AND DISCUSSION

In all the calculations presented in this paper great care has been taken to ensure that the results are accurate. The position at which infinity may be approximated varies with the value of the buoyancy parameter, λ, as does the mesh size that is required both normal and parallel to the plate. However, all the results presented in this paper are indistinguishable from those which may be obtained by taking smaller mesh sizes or taking infinity at a larger distance.

Figure 2 shows the numerically obtained value for

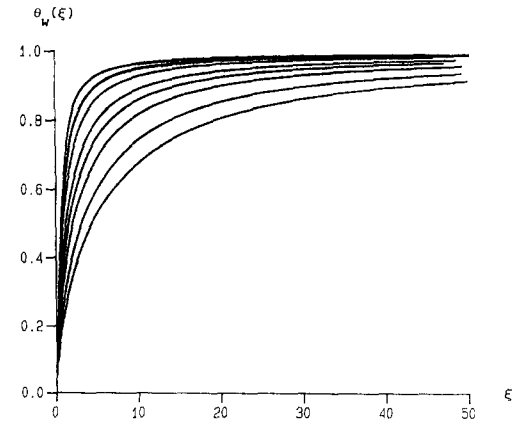

Fig. 2. Non-dimensional plate temperature $\theta_w(\xi)$ plotted against ξ for various values of $\lambda = -1, 0, 1, 5, 10, 20, 50$ and 100; as λ increases the curves decrease.

the wall temperature, $\theta_w(\xi)$, obtained using the method described in Section 3.3 and given by equation (30), as a function of the distance along the plate, $\xi = x^{1/2}$, for various values of $\lambda \geqslant -1$. It is seen that if the value of ξ is sufficiently large then the asymptotic value of $\theta_w(\xi) = 1$ is approached. As expected from the investigation of equations (27) and (28), the larger the value of λ the longer it is before the asymptotic value of $\theta_w(\xi)$ is attained. It should be noted that the calculations have been performed for sufficiently large values of ξ for the asymptotic value of $\theta_w(\xi)$ to have been obtained. However, because of the difficulty in clearly displaying all the important features of the behaviour of $\theta_w(\xi)$ over a wide range of values of the parameter λ, $\theta_w(\xi)$ is only displayed up to $\xi = 50$.

It is very important to observe from Fig. 2 that, when the direction of the fluid flow at large distances from the plate is in the opposite direction to the buoyancy force, i.e. $\lambda < 0$, it is possible to obtain a full solution of the governing parabolic partial differential equations (27) and (28) without the flow separating from the plate. In all other non-conjugate problems, which have been studied by numerous authors, where there is an opposing flow condition it is observed that the flow always separates when $\lambda < 0$. This situation is always found to hold for all inclinations of the plate in a porous medium (see refs. [9–11]) or a conventional fluid (see refs. [12, 13]).

Having obtained the temperature on the plate, $\theta_w(\xi)$, the next most important physical quantity to determine is the velocity on the plate, u_w. However, once $\theta_w(\xi)$ is known u_w is easily determined from equation (3) and is therefore not presented in detail in this paper. However, it is important to observe that, in the limit $\xi \to \infty$, as λ increases u_w increases.

Typical temperature profiles of the convective fluid, $\theta(\xi, \zeta)$, at various locations along the plate, ξ, are shown in Fig. 3 as a function of ζ, the scaled distance from the plate, for $\lambda = 1$. As the value of ξ increases the profile increases monotonically and tends to the fully developed one. Further, in Fig. 3 we again observe that $\theta_w(\xi)$ is initially zero but tends monotonically to unity. The results for other values of $\lambda \geqslant -1$ show a similar phenomena to those shown in Fig. 3 but the larger the value of λ the slower is the approach to the asymptotic solution. Again, the velocity profiles may easily be determined from the temperature profiles using equation (3).

In Fig. 4 the variation of $\theta_w(\xi)$ as a function of ξ is presented for $\lambda = 0.5$ [Fig. 4(a)], and $\lambda = -0.5$ [Fig. 4(b)] obtained from the full numerical solution as presented in Section 3.3 and given by expression (30). Also shown in Fig. 4 are the small x solution, $\theta_w^{(1)}$, given in equation (16), and the large x solution, $\theta_w^{(2)}$, given in equation (25). In the small x solution the first six terms in series (16) have been obtained and the results for one, three and six terms are presented. Clearly, as the number of terms increases the larger is the range of validity of the solution. It is observed from Fig. 4, and from calculations performed at other

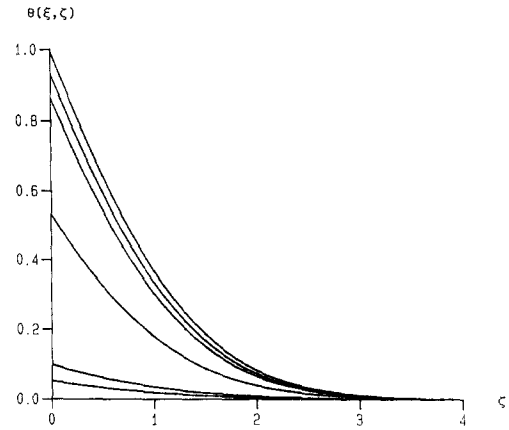

Fig. 3. Non-dimensional temperature profiles $\theta(\xi,\zeta)$ plotted against ζ at $\xi = 0.05, 0.1, 1, 5, 10$ and 100; as ξ increases the curves increase.

values of $\lambda \geqslant -1$, that the larger the value of λ the smaller is the range of validity of the small x solution, i.e. equation (16). In the large x solution (25) the first eigensolution (because of the leading-edge shift of the boundary-layer) comes in at the third term in series (21) and hence only the first two terms for large values of x have been calculated. Again, it is observed that the larger the value of λ the larger must the value of ξ be taken in order for there to be a good agreement between the series solution (25) and the full numerical solution (30). Thus, as seen from Fig. 4, the smaller the value of λ the larger is the range of values of ξ for which either the small or the large x solutions are valid.

When $\lambda < -1$ the fluid flow always separates from the plate. The reason for this is that $\theta_w(\xi)$ always increases monotically from zero at $x = 0$ to unity at large values of x, and, hence, if the velocity component along the plate, i.e. u_w, is to be always positive then we see from equation (3) that $\lambda \geqslant -1$. If $u > 0$ everywhere then information is always transmitted downstream of the leading edge of the plate and we therefore expect that we should be able to march from small values of x to large values of x. However, if there are regimes where $u < 0$, this implies that information is being transmitted upstream and therefore we cannot expect, mathematically or physically, to be able to specify information at small values of x and move to large values of x without encountering fluid separation.

In Fig. 5 the variation of $\theta_w(\xi)$ with ξ as obtained from the full numerical solution described in Section 3.3 is presented for various values of $\lambda < -1$. The termination of the curve corresponds to the value where the numerical solution terminated because of the upstream influence. Also shown in Fig. 5 are the solutions obtained from the small x solution given by equation (16) and clearly in this situation there are no large x solutions. In Fig. 5(a), we have $\lambda = -1.1$ and one, three and six terms have been used in expansions (12). As expected, as the number of terms increases

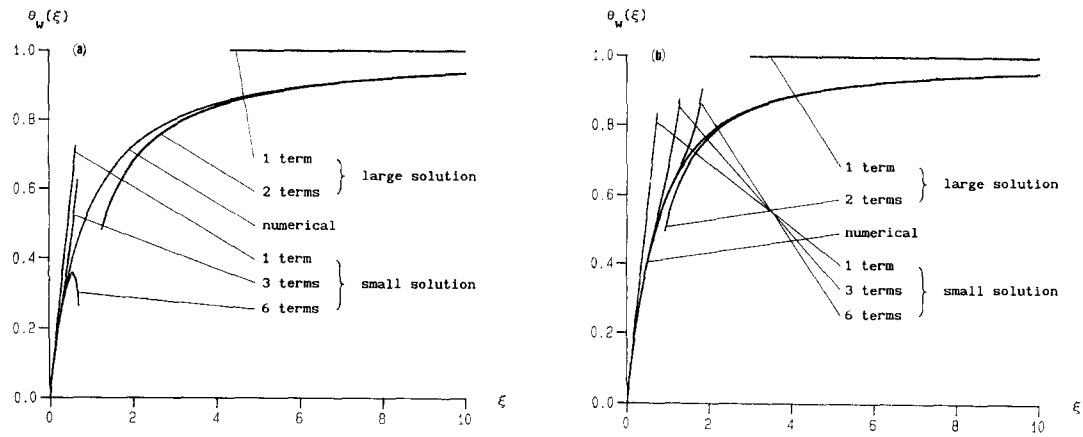

Fig. 4. Non-dimensional plate temperature $\theta_w(\xi)$ plotted against ξ for: (a) $\lambda = 0.5$, (b) $\lambda = -0.5$.

the larger is the range of values of ξ for which there is a good agreement between the small x solution and the numerical solution. For $\lambda \in \{-1.5, -1.4, -1.3, -1.2\}$ Fig. 5(b) shows the comparison between the numerical solution and the six-term small x solution. It is observed that the small x solution is a good approximation to the numerical solution for all values of ξ but, of course, where the numerical solution breaks down, due to the separation of the boundary layer, cannot be easily predicted from the series solution. Figure 5(c) and (d) shows the variation of $\theta_w(\xi)$ as a function of ξ for $\lambda \in \{-10, -5, -3, -2\}$ and $\lambda \in \{-100, -50, -20\}$, respectively. It is seen, as one would expect, that as the value of λ becomes larger the sooner the flow separates. Figure 5(c) and (d) suggests that, as $\lambda \to$

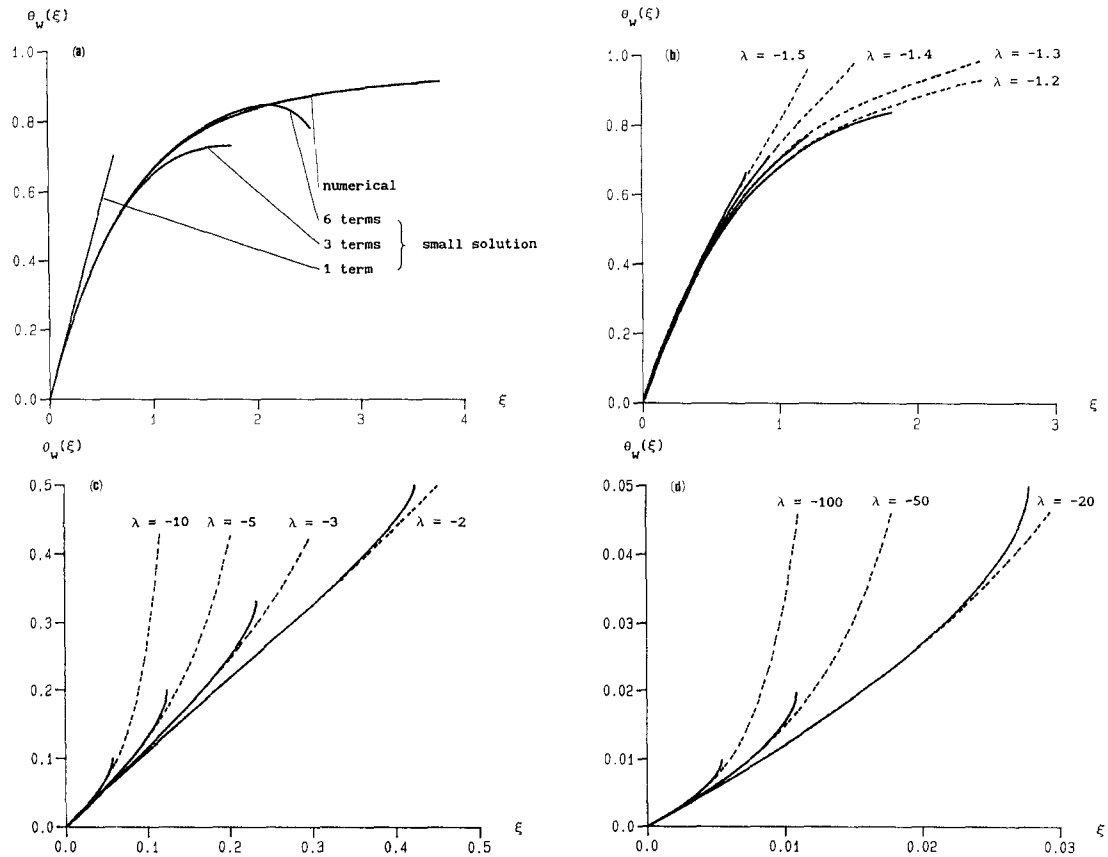

Fig. 5. Non-dimensional plate temperature $\theta_w(\xi)$ plotted against ξ for: (a) $\lambda = -1.1$; (b) $\lambda = -1.2, -1.3, -1.4$ and -1.5; (c) $\lambda = -2, -3, -5$ and -10; (d) $\lambda = -20, -30$ and -100. In cases (b)–(d) the solid lines represent the full numerical solution whilst the dashed lines represent the six-term expansion for the small solution.

$-\infty$, $\xi_{cr} \to 0$, where ξ_{cr} denotes the separation position of the boundary layer. Further, as the value of λ reduces from -1.5, the relative range over which the full numerical solution and the small x solution agree becomes smaller [see Fig. 5(c) and 5(d)].

Since the non-dimensional temperature is identically zero at $x = 0$ [see equation (8)] $u > 0$ at $x = 0$ and therefore it is always possible, for all finite values of λ, to be able to move away from $x = 0$. Further, we may expect that we will be able to continue the procedure until reversed flow starts. This will occur when [see equation (3)]

$$\theta = -1/\lambda \tag{31}$$

for the first time. In all the calculations we have performed we have found that the maximum temperature at any ξ location always occurs on the surface of the plate. Hence, condition (31) reduces to

$$\theta_w(\xi_{cr}) = -1/\lambda. \tag{32}$$

In Table 1 the location of the separation point, ξ_{cr}, and the corresponding 'separated' wall temperature, $\theta_w(\xi_{cr})$, obtained from the full numerical solution of equations (27) and (28) are presented for various values of $\lambda < -1$. The values of $-1/\lambda$ are also included in order to clarify the validity of condition (25) as to when the flow separates. Also, from Table 1, it is interesting to observe that the (critical) function t, defined as

$$t(\lambda) = \lambda \xi_{cr}(\lambda) \tag{33}$$

is a decreasing function of λ and it appears as though there is a finite limit for $t(\lambda)$ as $\lambda \to -\infty$, say t^0. This can be deduced from Table 1 where, for example, for large negative values of λ such as -100, -500 and -1000, the corresponding values of function t are very close to each other, namely, -0.539, -0.537 and -0.536, respectively. Therefore it appears that the value of -0.536 is probably very close to the correct asymptotic value of t^0. Because of the above observations we now introduce the approximate functions

$$t_j(\lambda) = \lambda \xi_{cr}^{(j)}(\lambda), \quad j \geqslant 1 \tag{34}$$

where $\xi_{cr}^{(j)}$ is the 'separation' point as predicted from the small x solution, given by equation (16), when using j terms in the expansion in order to satisfy condition (32). The values of $\xi_{cr}^{(j)}(\lambda)$ for $j \in \{1, 3, 6\}$ are also given in Table 1. Again, it can be observed that the values of $t_j(\lambda)$ for large negative values of λ are given by

$$t_j^0 = \begin{cases} -0.886 & \text{for } j = 1 \\ -0.650 & \text{for } j = 3 \\ -0.590 & \text{for } j = 6 \end{cases} \tag{35}$$

which appear to be approaching the limit t^0. At this stage it is worth noting that the values given by expression (35) can also be obtained by using the fact that, when λ becomes very large and negative, it can be removed from equations (14) through the transformations

$$f_j = \lambda^j F_j \tag{36a}$$

$$h_j = \lambda^j H_j. \tag{36b}$$

Equations (14) then become independent of λ and take the forms

$$F_j' = H_{j-1}$$

$$2H_j'' + F_0 H_j' - (j+1) F_0' H_j = \sum_{i=0}^{j-1} [(i+1) H_i F_{j-i}' - (i+2) F_{i+1} H_{j-i-1}']$$

$$F_j(0) = 0 \quad H_j'(0) = 0 \quad H_j(\infty) = 0 \tag{37}$$

with $j \geqslant 1$. Obviously $F_0 = f_0$ and $H_0 = h_0$, and hence F_0 and H_0 are given by equations (13). In solving equations (37) of major interest is the determination of the values $H_i(0)$, $i \geqslant 0$, since the temperature on the plate, $\theta_w^{(1)}(x)$, can be obtained using relation (16), via transformation (36b). From the analytical solution (15) it is easy to find that $H_0(0) = 2/\sqrt{\pi}$ and $H_1(0) = 1/4 - 2/\pi$, whilst the further values

Table 1. Location of the separation point and the corresponding 'separated' wall temperature for various values of $\lambda < -1$

$-\lambda$	ξ_{cr}	$\xi_{cr}^{(6)}$	$\xi_{cr}^{(3)}$	$\xi_{cr}^{(1)}$	$\theta_w(\xi_{cr})$	$-1/\lambda$
1.1	3.768	—	—	0.805	0.915	0.909
1.2	1.818	1.670	3.875	0.738	0.838	0.833
1.3	1.213	1.195	1.300	0.681	0.771	0.769
1.4	0.930	0.930	0.960	0.633	0.715	0.714
1.5	0.762	0.780	0.805	0.590	0.666	0.666
2	0.423	0.450	0.475	0.443	0.499	0.500
3	0.232	0.255	0.270	0.295	0.332	0.333
5	0.123	0.136	0.147	0.177	0.199	0.200
10	5.74E−2	6.35E−2	7.00E−2	8.86E−2	9.98E−2	0.100
20	2.77E−2	3.10E−2	3.30E−2	4.43E−2	4.98E−2	5.00E−2
30	1.18E−2	2.05E−2	2.20E−2	2.95E−2	3.31E−2	3.33E−2
50	1.08E−2	1.20E−2	1.35E−2	1.77E−2	1.97E−2	2.00E−2
100	5.39E−3	6.10E−3	6.60E−3	8.86E−3	9.87E−3	1.00E−2
500	1.07E−3	1.19E−3	1.30E−3	1.77E−3	1.98E−3	2.00E−3
1000	5.36E−4	5.90E−4	6.50E−4	8.86E−4	9.95E−4	1.00E−3

$H_2(0) = 0.338$, $H_3(0) = -0.383$, $H_4(0) = 0.490$, $H_5(0) = -0.677$, etc. have been obtained by numerically integrating equations (37). The coefficients $H_i(0)$, $i \geqslant 0$, are then introduced into equation (32) and the approximate limits t_j^0, $j \geqslant 1$, are obtained. The first six calculated values are

$$t_1^0 = -0.886 \quad t_2^0 = -0.712 \quad t_3^0 = -0.654 \quad (38a)$$

$$t_4^0 = -0.626 \quad t_5^0 = -0.608 \quad t_6^0 = -0.596. \quad (38b)$$

The agreement between these results and expression (35) is very good and was expected because for any value of λ it can be proved that $f_j(0)$ and $h_j(0)$ are polynomial functions in λ of degree j; hence, in the limit $\lambda \to -\infty$ only the leading coefficient is important and, in fact, this assumption was used in equations (36). In addition, from expressions (38) it is clear that the larger the value of j in the series expansions for small x the better does the limit t_j^0 approach the full numerical limit t^0, i.e. approximately -0.536. This convergence is shown more clearly in Fig. 6 through log–log plots of the critical values ξ_{cr}, $\xi_{cr}^{(1)}$, $\xi_{cr}^{(3)}$ and $\xi_{cr}^{(6)}$, as given in Table 1, against $-\lambda$. From Fig. 6 it is observed that the curves are parallel when $-\lambda$ is large and the full numerical curve is more closely approached by the inclusion of more terms in the series expansion for small values of x. Furthermore, it is likely that these curves are almost straight lines for large values of $-\lambda$, illustrating the convergence of t, t_1, t_3 and t_6. Finally, from the wide range of values $\lambda < -1$ which have been analysed in Figs. 5 and 6 and Table 1, it may be postulated that the small x solution is a good approximation *almost* up to the point of separation.

5. CONCLUSIONS

The problem of steady conjugate mixed convection along a vertical finite flat plate which is embedded in a porous medium has been studied. The conjugation parameter has been scaled out of the governing partial differential equations and the problem only contains the buoyancy parameter, λ. Numerical solutions of these equations were obtained for both aiding ($\lambda > 0$) and opposing ($\lambda < 0$) flows. In addition, small (near the leading edge) and large (downstream of the leading edge) solutions have been reported. A series of computations have been performed in which the principal parameters (the distance along the plate, ξ, and the buoyancy parameter, λ) which govern the heat transfer in this geometry have been systematically investigated. As a result, detailed relations between these parameters and the location where the flow separates from the plate have been elucidated. The finite-difference solutions have been proved to be accurate in comparison with the reported small and large series expansion solutions. The important effects of the buoyancy parameter λ on the temperature profiles at the plate and in the convective fluid have been discussed, and it is concluded that for $\lambda \geqslant -1$ there is always a solution of the boundary-layer equations, whilst for $\lambda < -1$ the flow separates at a position downstream of the leading edge of the plate. Thus, the *conjugate* nature of the problem has enabled solutions to be found for the opposing flow situation when $-1 \leqslant \lambda < 0$. Therefore, as mentioned in ref. [8], careful considerations should be given in the porous medium context to the problem of flow separation which results in the spreading of the heat supplied from the plate into a much wider region of the porous medium than the boundary layer on the plate.

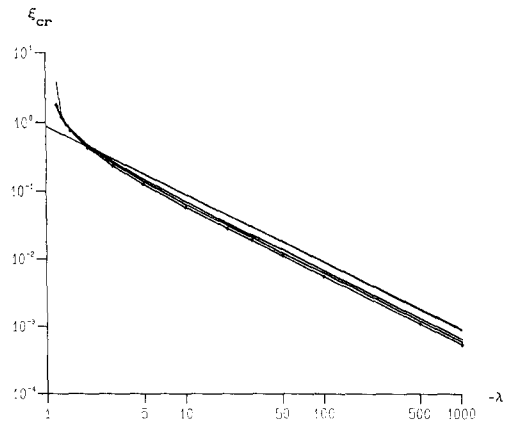

Fig. 6. Log–log plot curves of ξ_{cr} against $-\lambda$, as given by Table 1, using the full numerical solution (dotted line) and the one-, three and six-term expansions for the small solution (solid lines in decreasing order).

Acknowledgements—Professors I. Pop and D. B. Ingham would like to express their thanks to the EEC for some of the financial support for this project. Daniel Lesnic would also like to thank TEMPUS and ORS for their financial support.

REFERENCES

1. O. G. Martynenko and Yu A. Sokovishin, Buoyancy-induced heat transfer on a vertical non-isothermal surface. In *Heat Transfer Reviews*, Vol. 1, *Convective Heat Transfer* (Edited by O. G. Martynenko and A. A. Zukauskas). Hemisphere, Washington, DC (1989).
2. D. A. Nield and A. Bejan, *Convection in Porous Media*. Springer, New York (1992).
3. I. Pop and J. H. Merkin, Conjugate free convection on a vertical surface in a saturated porous medium, *Fluid Dyn. Res.* (in press).
4. I. Pop and D. B. Ingham, A note on conjugate forced convection boundary-layer flow past a flat plate, *Int. J. Heat Mass Transfer* **36**, 3873–3876 (1993).
5. P. Cheng, Combined free and forced boundary layer flows about inclined surfaces in a porous medium, *Int. J. Heat Mass Transfer* **20**, 807–814 (1977).
6. P. Cheng and C. T. Hsu, Higher-order approximations for Darcian free convective flow about a semi-infinite vertical flat plate, *J. Heat Transfer* **106**, 143–151 (1984).
7. J. H. Merkin, On solutions of the boundary-layer equation with algebraic decay, *J. Fluid Mech.* **88**, 309–321 (1978).
8. R. Hunt and G. Wilks, Continuous transformation computation of boundary-layer equations between similarity regimes, *J. Comp. Phys.* **40**, 478–490 (1981).

9. D. A. S. Rees and D. S. Riley, Free convection above a near horizontal semi-infinite heated surface embedded in a saturated porous medium, *Int. J. Heat Mass Transfer* **28,** 183–190 (1985).
10. D. B. Ingham, J. H. Merkin and I. Pop, Natural convection from a semi-infinite flat plate inclined at a small angle to the horizontal in a saturated porous medium, *Acta Mech.* **57,** 183–202 (1985).
11. J. H. Merkin, Mixed convection boundary-layer flow on a vertical surface in a saturated porous medium, *J. Engng Math.* **14,** 301–313 (1980).
12. D. R. Jones, Free convection from a semi-infinite flat plate inclined at a small angle to the horizontal, *Q. Jl Mech. Appl. Math.* **26,** 77–98 (1973).
13. T. S. Chen and B. F. Armaly, Mixed convection in external flow. In *Handbook of Single-phase Convective Heat Transfer* (Edited by S. Kakac, R. K. Shah and W. Aung), pp. 14.1–14.35. John Wiley, New York (1987).